

$\tau \rightarrow K_S \pi^- \nu_\tau$ and $\tau \rightarrow K^- \eta \nu_\tau$ decays: A combined analysis

ESCRIBANO R.^{1,2}

(1. *Grup de Física Teòrica, Departament de Física, Universitat Autònoma de Barcelona, E-08193 Bellaterra (Barcelona), Spain;*

2. *Institut de Física d'Altes Energies (IFAE), The Barcelona Institute of Science and Technology,*

Campus UAB, E-08193 Bellaterra (Barcelona), Spain)

Abstract: The decay spectra of $\tau^- \rightarrow K_S \pi^- \nu_\tau$ and $\tau^- \rightarrow K^- \eta \nu_\tau$ decays are studied in a combined analysis using a dispersive representation of the required vector and scalar form factors. The $K^*(1410)$ resonance parameters are extracted with improved precision as compared to previous studies, with the findings $M_{K^{*'}} = 1304 \pm 17$ MeV and $\Gamma_{K^{*'}} = 171 \pm 62$ MeV. Isospin violations in the form factor slopes are investigated as the $K^- \pi^0$ vector form factor enters the description of the decay $\tau^- \rightarrow K^- \eta \nu_\tau$. In this respect, the spectrum of the transition $\tau^- \rightarrow K^- \pi^0 \nu_\tau$ would be extremely useful.

Key words: tau decays; dispersive analysis; scalar and vector form factors; $K^*(1410)$ resonance; isospin violation

CLC number: O572.3 **Document code:** A doi:10.3969/j.issn.0253-2778.2016.05.007

Citation: ESCRIBANO R. $\tau \rightarrow K_S \pi^- \nu_\tau$ and $\tau \rightarrow K^- \eta \nu_\tau$ decays: A combined analysis[J]. Journal of University of Science and Technology of China, 2016, 46(5): 398-406.

$\tau \rightarrow K_S \pi^- \nu_\tau$ 和 $\tau \rightarrow K^- \eta \nu_\tau$ 衰变: 联合分析

ESCRIBANO R.^{1,2}

(1. 巴塞罗那自治大学物理系理论物理研究组, 巴塞罗那 E-08193, 西班牙;

2. 巴塞罗那自治大学高能物理研究所, 巴塞罗那 E-08193, 西班牙)

摘要: 利用所需的矢量和标量形状因子的色散表示, 综合分析了 $\tau \rightarrow K_S \pi^- \nu_\tau$ 和 $\tau \rightarrow K^- \eta \nu_\tau$ 衰变谱. 与先前的研究相比, 得到了更高精度的 $K^*(1410)$ 共振参数, $M_{K^{*'}} = 1304 \pm 17$ MeV 和 $\Gamma_{K^{*'}} = 171 \pm 62$ MeV. 由于 $K^- \pi^0$ 矢量形状因子与 $\tau^- \rightarrow K^- \eta \nu_\tau$ 衰变的描述有关, 对在形状因子斜率中同位旋的破缺进行了研究. 在这方面, $\tau^- \rightarrow K^- \pi^0 \nu_\tau$ 的跃迁谱将是极为有用的.

关键词: τ 衰变; 色散分析; 标量和矢量形状因子; $K^*(1410)$ 共振态; 同位旋破缺

Received: 2015-11-30; **Revised:** 2016-04-20

Foundation item: Supported in part by the the Ministerio de Ciencia e Innovación (FPA2011-25948), the Ministerio de Economía y Competitividad (CICYT-FEDER-FPA 2014-55613-P, SEV-2012-0234), the Secretaria d'Universitats i Recerca del Departament d'Economia i Coneixement de la Generalitat de Catalunya (2014 SGR 1450), and the Spanish Consolider-Ingénio 2010 Programme CPAN (CSD2007-00042).

Biography: ESCRIBANO R., male, born in 1969, PhD/associate Prof. Research field: phenomenology of strong interactions at low energies. E-mail: rescriba@ifae.es

0 Introduction

The dominant strangeness-changing τ decays are into $K\pi$ meson systems and the corresponding observables have been measured with increasing precision at LEP^[1-2], BaBar^[3] and Belle^[4]. We would like to note that the BaBar Collaboration published their analysis for the $K^- \pi^0$ mode^[3], while Belle studied the $K_S \pi^-$ decay channel^[4]. Belle's spectrum became publicly available but the published BaBar analysis only concerned the branching fraction while the corresponding spectrum has not been released yet. As a result, all dedicated studies of the $\tau^- \rightarrow (K\pi)^- \nu_\tau$ decays focused on the $K_S \pi^-$ system^[5-10]. Consequently, even using data from semileptonic Kaon decays ($K \rightarrow \pi l \nu$, so-called K_{l3} decays)^[9-10], important information on isospin breaking effects in the low-energy expansion of the hadronic form factors could not be extracted. The quoted references succeeded in improving the determination of the $K^*(892)$ and $K^*(1410)$ resonance properties: their pole positions and relative weight, although the errors on the radial excitation were noticeably larger than in the $K^*(892)$ case.

The threshold for the decay $\tau^- \rightarrow K^- \eta \nu_\tau$ is above the region of $K^*(892)$ -dominance which enhances its sensitivity to the properties of the heavier copy $K^*(1410)$. This observation was one of the motivations for the analysis of Ref. [11], where it was first shown that the considered decays were competitive to the $\tau^- \rightarrow (K\pi)^- \nu_\tau$ decays for the extraction of the $K^*(1410)$ meson parameters. This was made possible thanks to BaBar^[12] and Belle^[13] data of the $K^- \eta$ spectrum which improved drastically the pioneering CLEO^[14] and ALEPH^[15] measurements.

The main purpose of this work is to illustrate the potential of a combined analysis of the decays $\tau^- \rightarrow (K\pi)^- \nu_\tau$ and $\tau^- \rightarrow K^- \eta \nu_\tau$ in the determination of the $K^*(1410)$ resonance properties. This study is presently limited by three facts: unfolding of detector effects has not been performed for the

latter data, the associated errors of these are still relatively large and no measurement of the $K^- \pi^0$ spectrum has been published by the B-factories. We intend to demonstrate that an updated analysis of the $K_S \pi^-$ and/or $K^- \eta$ Belle spectrum including the whole Belle-I data sample could improve notably the knowledge of the $K^*(1410)$ pole position. Therefore, we hope that our paper strengthens the case for a (re)analysis of the $(K\pi)^-$ and $K^- \eta$ spectra at the first generation B-factories including a larger data sample and also for devoted analyses in the forthcoming Belle-II experiment. Turning to the low-energy parameters, we emphasize the importance of (independent) measurements of the two $\tau^- \rightarrow (K\pi)^- \nu_\tau$ charge channels with the target of disentangling isospin violations in forthcoming studies.

While the $K\pi$ -hadronization in the $\tau^- \rightarrow (K\pi)^- \nu_\tau$ decays is quite well understood, earlier analyses of $\tau^- \rightarrow K^- \eta \nu_\tau$ decays^[16-18] were at odds with Belle data (also^[19] showed discrepancies) which motivated the claim in Belle's paper^[13] that "further detailed studies of the physical dynamics in τ decays with η mesons are required", as also observed in Ref. [20] in a more general context. In Ref. [11], we showed that a simple Breit-Wigner parametrization of the dominating vector form factor lead to a rather poor description of the data, while more elaborated approaches based on Chiral Perturbation Theory (χPT)^[21-23] including resonances as dynamical fields^[24-25] and resumming final-state interactions (FSI) encoded in the chiral loop functions provided very good agreement with data.

1 Form factor representations

The required form factors cannot be computed analytically from first principles. Still, the symmetries of the underlying QCD Lagrangian are useful to determine their behaviour in specific limits, the chiral or low-energy limit and the high-energy behaviour, so that the model dependence is reduced to the interpolation between these known regimes. For our central fits, to be presented in

the next section, we follow the dispersive representation of the vector form factors outlined in Ref. [8], and briefly summarised below for the convenience of the reader. For the case of the $K_S\pi^-$ system, including two resonances, the $K^* = K^*(892)$ and the $K^{*'} = K^*(1410)$, the reduced vector form factor is taken to be of the form^[8]

$$\tilde{f}_+^{K\pi}(s) = \frac{m_{K^*}^2 - \kappa_{K^*} \tilde{H}_{K\pi}(0) + \gamma_S}{D(m_{K^*}, \gamma_{K^*})} - \frac{\gamma_S}{D(m_{K^{*'}}, \gamma_{K^{*'}})} \quad (1)$$

where

$$D(m_n, \gamma_n) = m_n^2 - s - \kappa_n \tilde{H}_{K\pi}(s) \quad (2)$$

and

$$\kappa_n = \frac{192\pi}{\sigma_{K\pi}(m_n^2)^3} \frac{\gamma_n}{m_n} \quad (3)$$

The fit function for the vector form factor is expressed in terms of the unphysical “mass” and “width” parameters m_n and γ_n . They are denoted by small letters, to distinguish them from the physical mass and width parameters M_n and Γ_n , which will later be determined from the pole positions in the complex plane and are denoted by capital letters. The scalar one-loop integral function $\tilde{H}_{K\pi}(s)$ is defined below Eq. (3) of Ref. [5], however removing the factor $1/f_\pi^2$ which cancels if κ_n is expressed in terms of the unphysical width γ_n . Finally, in Eq. (3), the phase space function $\sigma_{K\pi}(s)$ is given by $\sigma_{K\pi}(s) = 2q_{K\pi}(s)/\sqrt{s}$. Since the K^* resonances that are produced through the τ decay are charged, and can decay or rescatter into both $K^0\pi^-$ and $K^-\pi^0$ channels, in the resonance propagators described by Eqs. (1) to (3) we have chosen to employ the corresponding isospin average, that is

$$\tilde{H}_{K\pi}(s) = \frac{2}{3} \tilde{H}_{K^0\pi^-}(s) + \frac{1}{3} \tilde{H}_{K^-\pi^0}(s) \quad (4)$$

and analogously for $\sigma_{K\pi}(s)$, such that the resonance width contains both contributions. Little is known about a proper description of the width of the second vector resonance $K^{*'}$. The complicated $K^*\pi \sim K\pi\pi$ cuts may yield relevant effects which however necessitates a coupled-channel analysis like in Refs. [6, 10]. This is beyond the scope of

the present paper, in which for simplicity also for the second resonance only the two-meson cut is included. Similar remarks apply to a proper inclusion of the $K\eta$ and $K\eta'$ channels into Eq. (4) which would also require a coupled-channel analysis as was done for the corresponding scalar form factors in Refs. [26-27].

Next, we further follow Ref. [8] in writing a three-times subtracted dispersive representation for the vector form factor,

$$\tilde{f}_+^{K\pi}(s) = \exp\left[\alpha_1 \frac{s}{M_\pi^2} + \frac{1}{2}\alpha_2 \frac{s^2}{M_\pi^4} + \frac{s^3}{\pi} \int_{s_{K\pi}}^{s_{\text{cut}}} ds' \frac{\delta_1^{K\pi}(s')}{(s')^3 (s' - s - i^0)}\right] \quad (5)$$

where $s_{K\pi} = (M_K + M_\pi)^2$ is the $K\pi$ threshold and the two subtraction constants α_1 and α_2 are related to the slope parameters appearing in the low-energy expansion of the form factor:

$$\tilde{f}_+^{K\pi}(s) = 1 + \lambda'_+ \frac{s}{M_\pi^2} + \frac{1}{2} \lambda''_+ \frac{s^2}{M_\pi^4} + \frac{1}{6} \lambda'''_+ \frac{s^3}{M_\pi^6} + \dots \quad (6)$$

Explicitly, the relations for the linear and quadratic slope parameters λ'_+ and λ''_+ take the form:

$$\lambda'_+ = \alpha_1, \quad \lambda''_+ = \alpha_2 + \alpha_1^2 \quad (7)$$

The incentive for employing a dispersive representation for the form factor is that in this way the influence of the less-well known higher energy region is suppressed. The associated error can be estimated by varying the cut-off s_{cut} in the dispersive integral. In order to obtain the required input phase $\delta_1^{K\pi}(s)$, like in Ref. [8] we use the resonance propagator representation Eq. (1) of the vector form factor. The phase can then be calculated from the relation

$$\tan \delta_1^{K\pi}(s) = \frac{\text{Im} \tilde{f}_+^{K\pi}(s)}{\text{Re} \tilde{f}_+^{K\pi}(s)} \quad (8)$$

which completes our representation of the vector form factor $\tilde{f}_+^{K\pi}(s)$.

The scalar form factors that are required for a complete description of the decay spectra will be taken from the coupled-channel dispersive representation of Refs. [26-27]. In particular, for

the scalar $K\pi$ form factor, we employ the update presented in Ref. [28]. For the scalar $K\eta$ form factor, the result of the three-channel analysis described in section 4.3 of Ref. [27] is used, choosing specifically the solution corresponding to fit (6.10) of Ref. [26]. As a matter of principle, this is not fully consistent, since the employed $K\pi$ form factor was extracted from a two-channel analysis, only including the dominant $K\pi$ and $K\eta'$ channels. But as our numerical analysis shows, anyway the influence of the scalar $K\eta$ form factor is insignificant so that this inconsistency can be tolerated.

2 Joint fits to $\tau^- \rightarrow K_S \pi^- \nu_\tau$ and $\tau^- \rightarrow K^- \eta \nu_\tau$ Belle data

For the $\tau^- \rightarrow K_S \pi^- \nu_\tau$ decays, an unfolded distribution measured by Belle is available^[4]. The corresponding number of events is 53 113.21 (54 157.59 before unfolding) and the bin width 11.5 MeV. As discussed in the earlier analyses, the data points corresponding to bins 5, 6 and 7 are difficult to bring into accord with the theoretical descriptions and have thus been excluded from the minimisation. The first point has not been included either, since the centre of the bin lies below the $K_S \pi^-$ production threshold. Following a suggestion from the experimentalists, as in the previous analyses we have furthermore excluded data corresponding to bin numbers larger than 90.

On the other hand, the published $\tau^- \rightarrow K^- \eta \nu_\tau$ Belle data^[13] are only available still folded with detector effects. Lacking for a better alternative, we have assumed that the $K^- \eta$ unfolding function is reasonably estimated by the $K_S \pi^-$ one and we have extracted in this way pseudo-unfolded data that we employed in our analysis. The corresponding number of events turns out 1 271.51 for a bin width of 25 MeV. In this case, we excluded the first three data points, which lie below the $K^- \eta$ production threshold, and discarded data above the τ mass.

Therefore, the number of fitted data points is

86 (28) for the $K_S \pi^- (K^- \eta)$ spectrum, together with the respective branching fractions; hence 116 data points in total. While it is possible to obtain stable fits without using the $K_S \pi^-$ branching fraction as a data point, this is not the case for the $K^- \eta$ channel. This is due to the fact that there are strong correlations between the branching ratio and the slope parameters of the vector form factor. While in the $K_S \pi^-$ case sufficiently many data points with small enough errors are available to determine all fit quantities from the spectrum, for the $K^- \eta$ decay mode this was not possible. As a consistency check, we will be comparing the fitted values of the respective branching ratios to the corresponding results obtained by directly integrating the spectrum in all our fits.

The fitted parameters within the dispersive representation of the form factors of Eq. (5) then include:

① The respective branching fractions $\overline{B}_{K\pi}$ and $\overline{B}_{K\eta}$. For consistency, we employ the results obtained by Belle in correspondence with the employed decay distribution data: $(0.404 \pm 0.013)\%$ ^[4] as well as $(1.58 \pm 0.10) \times 10^{-4}$ ^[13], respectively. This may be compared to the averages by the Particle Data Group, $(0.420 \pm 0.020)\%$ and $(1.52 \pm 0.08) \times 10^{-4}$ ^[29] and Heavy Flavour Averaging Group values^[30], $(0.410 \pm 0.009)\%$ and $(1.53 \pm 0.08) \times 10^{-4}$.

② The slope parameters: $\lambda'_{K\pi}$ and $\lambda'_{K\eta}$. As was noted in Ref. [11], while the former ones correspond to the $K_S \pi^-$ channel, the latter ones are related to the $K^- \pi^0$ system. Therefore, small differences in these parameters due to isospin violations are expected, and in the most general fit we allow for independent parameters in the two channels. As consistency checks of our procedure, we have also considered some fits assuming $\lambda'_{K\eta} = \lambda'_{K\pi}$. The findings of Ref. [8],

$$\lambda'_{K\pi} = (24.66 \pm 0.77) \times 10^{-3}$$

and

$$\lambda''_{K\pi} = (11.99 \pm 0.20) \times 10^{-4},$$

should serve as a reference point for our present

study, where however $\overline{B}_{K\tau}$ was fixed to the average $(0.418 \pm 0.011)\%$ at that time.

③ The pole parameters of the K^* (892) and K^* (1410) resonances. The masses and widths of these resonances are extracted from the complex pole position s_R according to $\sqrt{s_R} = M_R - \frac{i}{2}\Gamma_R$ ^[31].

For the lowest-lying resonance our results for the pole mass and width should be compatible with (892.0 ± 0.2) MeV and (46.2 ± 0.4) MeV^[9], respectively, where the quoted uncertainties are only statistical. We expect that the extraction of the K^* (1410) pole position should benefit from our present combined fit for which (1273 ± 75) MeV and (185 ± 74) MeV were obtained in Ref. [8] when the uncertainties are symmetrized.

④ The relative weight γ of the two resonances. In our isospin-symmetric way (1) of parametrizing the resonance propagators in the form factor description, γ should be the same for the $K_S\pi^-$ and $K^-\eta$ channels, which we shall assume for our central fit. Still, we have also tried to fit them independently, as differences might indicate inelastic or coupled-channel effects. As is

seen below, our various fit results do not show a sizeable preference for this possibility which supports our choice $\gamma_{K\eta} = \gamma_{K\tau}$. Our findings may be compared to the value $\gamma = -0.039 \pm 0.020$ of Ref. [8] indicating the influence of including the $\tau^- \rightarrow K^-\eta\nu_\tau$ mode into our analysis.

In Tab. 1, we display our results using slightly different settings, though in all of them Eq. (8) is employed to obtain the input phaseshift for the dispersion relation (5) and s_{cut} is fixed to 4 GeV² (the uncertainty associated to its variation is discussed later on): our reference fit (second column) corresponds to fixing $\gamma_{K\tau} = \gamma_{K\eta}$, fit A (third column) assumes $\lambda'_{K\tau} = \lambda'_{K\eta}$, fit B (fourth column) is the result of letting all parameters float independently and finally, fit C (fifth column) enforces both restrictions $\gamma_{K\tau} = \gamma_{K\eta}$ and $\lambda'_{K\tau} = \lambda'_{K\eta}$. It is seen that our approach is rather stable against these variations, as the $\chi^2/\text{n. d. f.}$ remains basically the same for the different scenarios. Also the values of the fitted parameters are always compatible across all fits. The largest modification is observed in fit A, where we fix $\lambda'_{K\tau} = \lambda'_{K\eta}$, but allow for independent resonance mixing parameters

Tab. 1 Fit results for different choices regarding linear slopes and resonance mixing parameters at $s_{\text{cut}} = 4$ GeV²

fitted value	reference fit	fit A	fit B	fit C
$\overline{B}_{K\tau}$ (%)	0.404 ± 0.012	0.400 ± 0.012	0.404 ± 0.012	0.397 ± 0.012
$(B_{K\tau}^{\#})$ (%)	(0.402)	(0.394)	(0.400)	(0.394)
M_{K^*}	892.03 ± 0.19	892.04 ± 0.19	892.03 ± 0.19	892.07 ± 0.19
Γ_{K^*}	46.18 ± 0.42	46.11 ± 0.42	46.15 ± 0.42	46.13 ± 0.42
$M_{K^{*'}}$	1305^{+15}_{-18}	1308^{+16}_{-19}	1305^{+15}_{-18}	1310^{+14}_{-17}
$\Gamma_{K^{*'}}$	168^{+52}_{-44}	212^{+66}_{-54}	174^{+58}_{-47}	184^{+56}_{-46}
$\gamma_{K\tau} \times 10^2$	$= \gamma_{K\eta}$	$-3.6^{+1.1}_{-1.5}$	$-3.3^{+1.0}_{-1.3}$	$= \gamma_{K\eta}$
$\lambda'_{K\tau} \times 10^3$	23.9 ± 0.7	23.6 ± 0.7	23.8 ± 0.7	23.6 ± 0.7
$\lambda''_{K\tau} \times 10^4$	11.8 ± 0.2	11.7 ± 0.2	11.7 ± 0.2	11.6 ± 0.2
$\overline{B}_{K\eta} \times 10^4$	1.58 ± 0.10	1.62 ± 0.10	1.57 ± 0.10	1.66 ± 0.09
$(B_{K\eta}^{\#}) \times 10^4$	(1.45)	(1.51)	(1.44)	(1.58)
$\gamma_{K\eta} \times 10^2$	$-3.4^{+1.0}_{-1.3}$	$-5.4^{+1.8}_{-2.6}$	$-3.9^{+1.4}_{-1.7}$	$-3.7^{+1.0}_{-1.4}$
$\lambda'_{K\eta} \times 10^3$	20.9 ± 1.5	$= \lambda'_{K\tau}$	21.2 ± 1.7	$= \lambda'_{K\tau}$
$\lambda''_{K\eta} \times 10^4$	11.1 ± 0.4	11.7 ± 0.2	11.1 ± 0.4	11.8 ± 0.2
$\chi^2/\text{n. d. f.}$	$108.1/105 \sim 1.03$	$109.9/105 \sim 1.05$	$107.8/104 \sim 1.04$	$111.9/106 \sim 1.06$

【Note】 See the main text for further details. Dimensional parameters are given in MeV. As a consistency check, for each of the fits we provide (in brackets) the value of the respective integrated branching fractions.

γ . This is partly expected since in the reference fit the former equality on the slope parameters is only fulfilled at the 2σ level. Letting all parameters float in fit B yields results which are nicely compatible with the reference fit, though for some parameters resulting in slightly larger uncertainties. Finally, enforcing both, the linear slopes as well as the mixing parameters to be equal also results in a compatible fit where now the largest shift by about 2σ is found in $\lambda''_{K\eta}$.

For presenting our final results, we have added to the statistical fit error a systematic uncertainty due to the variation of s_{cut} . To this end, we have taken the largest variation of central values while varying s_{cut} (which is always found at $s_{\text{cut}} = 3.24 \text{ GeV}^2$) and have added this variation in quadrature to the statistical uncertainty. We then obtain

$$\left. \begin{aligned} \bar{B}_{K\pi} &= (0.404 \pm 0.012)\%, \\ M_{K^*} &= 892.03 \pm 0.19, \Gamma_{K^*} = 46.18 \pm 0.44, \\ M_{K^{*'}} &= 1305^{+16}_{-18}, \Gamma_{K^{*'}} = 168^{+65}_{-59}, \\ \gamma_{K\pi} &= \gamma_{K\eta} = (-3.4^{+1.2}_{-1.4}) \times 10^{-2}, \\ \lambda'_{K\pi} &= (23.9 \pm 0.9) \times 10^{-3}, \\ \lambda''_{K\pi} &= (11.8 \pm 0.2) \times 10^{-4}, \\ \lambda'_{K\eta} &= (20.9 \pm 2.7) \times 10^{-3}, \\ \lambda''_{K\eta} &= (11.1 \pm 0.5) \times 10^{-4}, \\ \bar{B}_{K\eta} &= (1.58 \pm 0.10) \times 10^{-4} \end{aligned} \right\} \quad (9)$$

were like before all dimensional quantities are given in MeV. Our final fit results are compared to the measured Belle $\tau^- \rightarrow K_S \pi^- \nu_\tau$ and $\tau^- \rightarrow K^- \eta \nu_\tau$ distributions^[4,13] in Fig. 1. Satisfactory agreement with the experimental data, in accord with the observed $\chi^2/\text{n. d. f.}$ of order one, is seen for all data points. The $K\pi$ spectrum is dominated by the contribution of the $K^*(892)$ resonance, whose peak is neatly visible. The scalar form factor contribution, although small in most of the phase space, is important to describe the data immediately above threshold. There is no such clear peak structure for the $K\eta$ channel as a consequence of the interplay between both K^*

resonances. The corresponding scalar form factor in this case is numerically insignificant.

Several comments regarding our final results of Eq. (9) and the reference fit of Tab. 1 are in order:

① Concerning the branching fractions, we observe that in the $K_S \pi^-$ channel our fit value $\bar{B}_{K\pi}$, which is mainly driven by the explicit input, and the result when integrating the fitted spectrum $B_{K\pi}^{\text{fit}}$, are in very good agreement, pointing to a satisfactory description of the experimental data. On the other hand, for the $K\eta$ case, one notes a trend that the integrated branching fraction $B_{K\eta}^{\text{fit}}$ turns out about 10% smaller than the fit result $\bar{B}_{K\eta}$, which points to slight deficiencies in the theoretical representation of this spectrum. This issue should be investigated further in the future with more precise data.

② The $K_S \pi^-$ slope parameters are well compatible with previous analogous analysis^[8-9]. For the corresponding $K^- \eta$ slopes, we obtain somewhat smaller values, which are, however, compatible with the crude estimates in Ref. [11]. The fact that the $K^- \eta$ slopes are about 2σ lower than the $K_S \pi^-$ slopes could be an indication of isospin violations, or could be a purely statistical effect. (Or a mixture of both.) To tackle this question and make further progress to disentangle isospin violations in the $K\pi$ form factor slopes, it is indispensable to study the related distribution for the $\tau^- \rightarrow K^- \pi^0 \nu_\tau$ decay, and the experimental groups should make every effort to also publish the corresponding spectrum for this process.

③ The pole parameters of the $K^*(892)$ resonance are in nice accord with previous values^[8-9] and have similar statistical fit uncertainties, which is to be expected as these parameters are driven by the data of the $\tau^- \rightarrow K_S \pi^- \nu_\tau$ decay, which was the process analysed previously. Regarding the parameters of the $K^*(1410)$ resonance, adding the $\tau^- \rightarrow K^- \eta \nu_\tau$ spectral data into the fit results in a substantial improvement in the determination of the mass, while only a slight

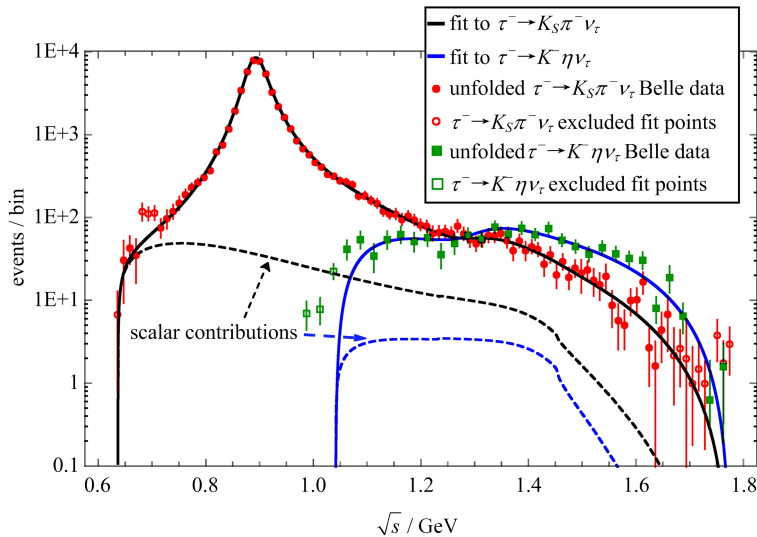


Fig. 1 Belle $\tau^- \rightarrow K_S \pi^- \nu_\tau$ (red solid circles)^[4] and $\tau^- \rightarrow K^- \eta \nu_\tau$ (green solid squares)^[13] measurements as compared to our best fit results (solid black and blue lines, respectively) obtained in combined fits to both data sets, as presented in Eq. (9). Empty circles (squares) correspond to data points which have not been included in the analysis. The small scalar contributions have been represented by black and blue dashed lines showing that while the former plays a role for the $K\pi$ spectrum close to threshold, the latter is irrelevant for the $K\eta$ distribution

improvement in the width is observed. Part of the large uncertainty in the width of the second K^* resonance can be traced back to the strong fit correlation with the mixing parameter γ , which is also not very well determined. Future data of either $\tau^- \rightarrow (K\pi)^- \nu_\tau$ or $\tau^- \rightarrow K^- \eta \nu_\tau$ hadronic invariant mass distributions should enable a more precise evaluation.

3 Conclusion

Hadronic decays of the τ lepton remain an advantageous tool for the investigation of the hadronization of QCD currents in the non-perturbative regime of the strong interaction. In this contribution to the proceedings, based on the original work published in Ref. [32], we have explored the benefits of a combined analysis of the $\tau^- \rightarrow K_S \pi^- \nu_\tau$ and $\tau^- \rightarrow K^- \eta \nu_\tau$ decays. This study was motivated by (our) separate earlier works on the two decay modes considering them as independent data sets. In particular, it was noticed in Ref. [11] that the $K\eta$ decay channel was rather sensitive to the properties of the $K^*(1410)$ resonance as the higher-energy region is less

suppressed by phase space.

Our description of the dominant vector form factor follows the work of Ref. [8], and proceeds in two stages. First, we write a Breit-Wigner type representation (1) which also fulfils constraints from χ PT at low-energies. In Eq. (1), we have resumed the real part of the loop function in the resonance denominators, but as was discussed above, employing the following dispersive treatment, this is not really essential. It mainly entails a shift in the unphysical mass and width parameters m_n and γ_n . Second, we extract the phase of the vector form factor according to Eq. (8) and plug it into the three-times subtracted dispersive representation of Eq. (5). This way, the higher-energy region of the form factor, which is less well known, is suppressed, and the form factor slopes emerge as subtraction constants of the dispersion relation. A drawback of this description is that the form factor does not automatically satisfy the expected $1/s$ fall-off at very large energies. Still, in the region of the τ mass (and beyond), our form-factor representation is a decreasing function such that the deficit should be

admissible without explicitly enforcing the short-distance constraint, thereby leaving more freedom for the slope parameters to assume their physical values.

In our combined dispersive analysis of the $(K\pi)^-$ and $K^-\eta$ decays we are currently limited by three facts; there are only published measurements of the $K_S\pi^-$ spectrum (and not of the corresponding $K^-\pi^0$ channel), the available $K^-\eta$ spectrum is not very precise and the corresponding data are still convoluted with detector effects. The first restriction prevents us from cleanly accessing isospin violations in the slope parameters of the vector form factor. From our joint fits, we have however managed to get an indication of this effect. The second one constitutes the present limitation in determining the $K^*(1410)$ resonance parameters but one should be aware that our approach to avoiding the last one (assuming that the $K_S\pi^-$ unfolding function gives a good approximation to the one for the $K^-\eta$ case) adds a small (uncontrolled) uncertainty to our results that can only be fixed by a dedicated study of detector resolution and efficiency. In this respect it would be most beneficial, if unfolded measured spectra would be made available by the experimental groups, together with the corresponding bin-to-bin correlation matrices.

In Tab. 1, we have compared slightly different options to implement constraints from isospin into the fits. Our reference fit is given by the second column of Tab. 1 and adding together the statistical fit uncertainties with systematic errors from the variation of s_{cut} , our final results are summarised in Eq. (9). The pole position we find for the $K^*(892)$ resonance is in perfect agreement with previous studies. The main motivation of this work was, however, to exploit the synergy of the $K\pi$ and $K\eta$ decay modes in characterizing the $K^*(1410)$ meson. According to our results, the relative weight γ of both vector resonances is compatible in the $K\pi$ and $K\eta$ vector form factors, which supports our assumption of their

universality. With current data we succeed in improving the determination of the $K^*(1410)$ pole mass, but regarding the width, substantial uncertainties remain. Our central result for these two quantities is

$$\left. \begin{aligned} M_{K^{*'}} &= (1304 \pm 17) \text{MeV}, \\ \Gamma_{K^{*'}} &= (171 \pm 62) \text{MeV} \end{aligned} \right\} \quad (10)$$

where we have symmetrized the uncertainties listed in Eq. (9).

References

- [1] BARATE R, DECAMP D, GHEZ P, et al (ALEPH Collaboration). Study of τ decays involving kaons, spectral functions and determination of the strange quark mass[J]. Eur Phys J C, 1999, 11: 599-618.
- [2] ABBIENDI G, AINSLEY C, ÅKESSON P F, et al (OPAL Collaboration). Measurement of the strange spectral function in hadronic τ decays[J]. Eur Phys J C, 2004, 35: 437-455.
- [3] AUBERT B, BONA M, BOUTIGNY D, et al (BaBar Collaboration). Measurement of the $\tau^- \rightarrow K^- \pi^0 \nu_\tau$ branching fraction[J]. Phys Rev D, 2007, 76:051104(R).
- [4] EPIFANOV D, ADACHI I, AIHARA H, et al (Belle Collaboration). Study of $\tau^- \rightarrow K_S \pi^- \nu_\tau$ decay at Belle [J]. Phys Lett B, 2007, 654: 65-73.
- [5] JAMIN M, PICH A, PORTOLÉS J. Spectral distribution for the decay $\tau \rightarrow \nu_\tau K \pi$ [J]. Phys Lett B, 2006, 640: 176-181.
- [6] MOUSSALLAM B. Analyticity constraints on the strangeness changing vector current and applications to $\tau \rightarrow K \pi \nu_\tau$, $\tau \rightarrow K \pi \pi \nu_\tau$ [J]. Eur Phys J C, 2008, 53: 401-412.
- [7] JAMIN M, PICH A, PORTOLÉS J. What can be learned from the Belle spectrum for the decay $\tau^- \rightarrow \nu_\tau K_S \pi^-$ [J]. Phys Lett B, 2008, 664:78-83.
- [8] BOITO D R, ESCRIBANO R, JAMIN M. $K\pi$ vector form-factor, dispersive constraints and $\tau \rightarrow \nu_\tau K \pi$ decays [J]. Eur Phys J C, 2009, 59: 821-829.
- [9] BOITO D R, ESCRIBANO R, JAMIN M. $K\pi$ vector form factor constrained by $\tau \rightarrow K \pi \nu_\tau$ and K_{l3} decays [J]. JHEP, 2010, 1009: 031.
- [10] BERNARD V. First determination of $f_+(0) |V_{us}|$ from a combined analysis of $\tau \rightarrow K \pi \nu_\tau$ decay and πK scattering with constraints from K_{l3} decays [J]. JHEP, 2014, 1406: 082.
- [11] ESCRIBANO R, GONZALEZ-SOLIS S, ROIG P. $\tau^- \rightarrow K^- \eta(\prime) \nu_\tau$ decays in chiral perturbation theory with resonances [J]. JHEP, 2013, 1310: 039.

- [12] DEL AMO SANCHEZ P, LEES J P, POIREAU V, et al (BaBar Collaboration). Studies of $\tau^- \rightarrow \eta K^- \nu_\tau$ and $\tau^- \rightarrow \eta \pi^- \nu_\tau$ at BaBar and a search for a second-class current[J]. Phys Rev D, 2011, 83: 032002.
- [13] INAMI K, OHSHIMA T, KAJIET H, et al (Belle Collaboration). Precise measurement of hadronic τ decays with an η meson[J]. Phys Lett B, 2009, 672: 209-218.
- [14] BARTELT J, CSORNA S E, JAIN V, et al (CLEO Collaboration). First observation of the decay $\tau^- \rightarrow K^- \eta \nu_\tau$ [J]. Phys Rev Lett, 1996, 76: 4 119.
- [15] BUSKULIC D, DE BONIS I, DECAMP D, et al (ALEPH Collaboration). A study of τ decays involving η and ω mesons[J]. Z Phys C, 1997, 74: 263-273.
- [16] PICH A. "Anomalous" η production in τ decay[J]. Phys Lett B, 1987, 196: 561-565.
- [17] BRAATEN E, OAKES R J, TSE S M. An effective Lagrangian calculation of the semileptonic decay modes of the τ lepton[J]. Int J Mod Phys A, 1990, 5: 2 737-2 753.
- [18] LI B A. Theory of τ mesonic decays[J]. Phys Rev D, 1997, 55: 1 436-1 452.
- [19] KIMURA D, LEE K Y, MOROZUMI T. The form factors of $\tau \rightarrow K\pi(\eta)\nu$ and the predictions for CP violation beyond the standard model[J]. Prog Theor Exp Phys, 2013, 2013: 053B03.
- [20] ACTIS S, ARBUZOV A, BALOSSINI G, et al. Quest for precision in hadronic cross sections at low energy: Monte Carlo tools vs. experimental data[J]. Eur Phys J C, 2010, 66: 585-686.
- [21] WEINBERG S. Phenomenological Lagrangians [J]. Physica A, 1979, 96: 327-340.
- [22] GASSER J, LEUTWYLER H. Chiral perturbation theory to one loop [J]. Annals Phys, 1984, 158: 142-210.
- [23] GASSER J, LEUTWYLER H. Chiral perturbation theory: Expansions in the mass of the strange quark [J]. Nucl Phys B, 1985, 250: 465-516.
- [24] ECKER G, GASSER J, PICH A, et al. The role of resonances in chiral perturbation theory[J]. Nucl Phys B, 1989, 321:311-342.
- [25] ECKER G, GASSER J, LEUTWYLER H, et al. Chiral Lagrangians for massive spin-1 fields[J]. Phys Lett B, 1989, 223: 425-432.
- [26] JAMIN M, OLLER J A, PICH A. S-wave $K\pi$ scattering in chiral perturbation theory with resonances [J]. Nucl Phys B, 2000, 587: 331-362.
- [27] JAMIN M, OLLER J A, PICH A. Strangeness changing scalar form-factors[J]. Nucl Phys B, 2002, 622: 279-308.
- [28] JAMIN M, OLLER J A, PICH A. Scalar $K\pi$ form factor and light quark masses[J]. Phys Rev D, 2006, 74: 074009.
- [29] BERINGER J, ARGUIN J F, BARNETT R M, et al (Particle Data Group). Review of particle physics (RPP) [J]. Phys Rev D, 2012, 86: 010001.
- [30] AMHIS Y, BANERJEE Sw, BERNHARD R, et al (Heavy Flavor Averaging Group). Averages of b-hadron, c-hadron, and tau-lepton properties as of early 2012[DB/OL]. arXiv:1207.1158 [hep-ex].
- [31] ESCRIBANO R, GALLEGOS A, LUCIO M J L, et al. On the mass, width and coupling constants of the $f_0(980)$ [J]. Eur Phys J C, 2003, 28: 107-114.
- [32] ESCRIBANO R, GONZÁLEZ-SOLÍS S, JAMIN M, et al. Combined analysis of the decays $\tau^- \rightarrow K_S \pi^- \nu_\tau$ and $\tau^- \rightarrow K^- \eta \nu_\tau$ [J]. JHEP, 2014, 1409: 042.